1-1-2020

Leak location based on PDS-VMD of leakage-induced vibration signal under low SNR in water-supply pipelines

Shuaiyong Li

Chuanqiang Xia

Zhenhua Cheng

Weipei Mao

Ying Liu
Edith Cowan University

See next page for additional authors

10.1109/ACCESS.2020.2984640

Li, S., Xia, C., Cheng, Z., Mao, W., Liu, Y., & Habibi, D. (2020). Leak location based on PDS-VMD of leakage-induced vibration signal under low SNR in water-supply pipelines. *IEEE Access, 8*, 68091-68102. https://doi.org/10.1109/ACCESS.2020.2984640

IEEE Access
Multidisciplinary | Rapid Review | Open Access Journal

Received March 22, 2020, accepted March 27, 2020, date of publication March 31, 2020, date of current version April 22, 2020.

Digital Object Identifier 10.1109/ACCESS.2020.2984640

Leak Location Based on PDS-VMD of Leakage-Induced Vibration Signal Under Low SNR in Water-Supply Pipelines

SHUAIYONG LI[1], CHUANQIANG XIA[1], ZHENHUA CHENG[1], WEIPEI MAO[1], YING LIU[2,3], AND DARYOUSH HABIBI[2]

[1]Key Laboratory of Industrial Internet of Things and Networked Control, Ministry of Education, Chongqing University of Posts and Telecommunications, Chongqing 400065, China
[2]School of Engineering, Edith Cowan University, Joondalup, WA 6027, Australia
[3]State Key Laboratory of Acoustics, Institute of Acoustics, Chinese Academy of Sciences, Beijing 100190, China

Corresponding author: Shuaiyong Li (lishuaiyong@cqupt.edu.cn)

This work was supported in part by the National Natural Science Foundation Project of China under Grant 61703066, in part by the Natural Science Foundation Project of Chongqing under Grant cstc2018jcyjAX0536, in part by the Chongqing Special Project of Technology Innovation and Application Development under Grant cstc2018jszx-cyztzxX0028, Grant cstc2019jscx-fxydX0042, and Grant cstc2019jscx-zdztzxX0053.

ABSTRACT Leak location in water-supply pipelines is of great significance in order to preserve water resources and reduce economic losses. Cross-correlation (CC) based leak location is a popular and effective method in water-supply pipelines (WSP). However, with a decrease of signal to noise ratio (SNR), the errors of time-delay estimation (TDE) based on CC will become larger making it almost impossible to determine a leakage position. Hence, this work proposes leak location based on a combination of phase difference spectrum and variational mode decomposition (PDS-VMD) of leakage-induced vibration signal under low SNR for WSP. Firstly, the leakage-induced vibration signal is decomposed into several intrinsic mode functions (IMFs) by VMD, where the characteristic frequency band is determined by PDS of cross spectrum of two leakage signals. Then, the energy ratio of leakage signal in characteristic frequency band serves as a guideline to select effective IMF components from the decomposed IMFs. Finally, the selective IMFs are reconstituted into a new signal which can be used to determine a leak position using CC based TDE. In order to verify the effectiveness of the proposed leak location algorithm, the method based on PDS-VMD is compared with that using CC, combination of CC coefficient and VMD (CCC-VMD) using both simulation and experiment. The simulation and experimental results demonstrate that the proposed PDS-VMD method is more suitable for leak location in WSP, which provides immunity to both broadband and narrow band noise under low SNR.

INDEX TERMS VMD, cross-spectral analysis, leakage location, low SNR, water supply pipeline.

I. INTRODUCTION

Leakage in water-supply pipelines results in economic losses from water wastage and serves as a health risk since leaks are potential entry points for contaminants during low pressure intrusion events [1]. Hence, it is necessary to conduct research on leak location for WSP to guarantee safe and reliable operation of WSP [2]–[4]. So far, much research has been conducted for leak detection and location methods in WSP. Since 1991, vibration-based leak detection method has been used for WSP, where the vibration signal can be acquired by either accelerometers or hydrophones at two access points, on either side of a suspected leak. Leak location based on CC analysis of vibration signal developed by Fuchs and Riehle over the last 30 years is regarded as one of most popular and effective technology in WSP [5]–[13], which has been widely used to locate leaks in buried WSP. In real leak location practice, the SNR of acquired data by accelerometers or hydrophones is very low as result of traffic, mechanical devices, turbulence, etc., which directly influence the correlation-based time delay estimator resulting in a larger leak location error. The enhancement of signal to noise

The associate editor coordinating the review of this manuscript and approving it for publication was Jinming Wen.

ratio (SNR) by suppressing environmental noise in collected data is essential to ensure reliability of leak detection and reduce leak location error.

TDE can be used to enhance SNR of leak signals and reduce leak location errors [8]. The generalized cross correlation (GCC) can be obtained by pre-filtering the leak signal prior to performing the CC method, which enhances the signals in the frequency bands where the SNR is high, thereby suppressing the signal outside these frequency bands. Knapp and Carter have discussed the characteristics of five GCC methods and compared them with the CC method [14]. The GCC can sharpen the peak of CC function by pre-whitening the leak signals whose frequency bands must be extracted. However, it is difficult to determine the frequency bands of leak signals in various pipeline situation (pipeline material, pressures, leakage apertures, etc.) and surroundings (soil, temperature, climate etc.), which results in an inability to design a pre-filter for GCC to improve SNR of leak signals. Thus, the GCC based leak location method will still have a larger error for WSP.

To overcome this weakness of GCC, adaptive TDE based on least mean square (LMS) error is applied in leak location for WSP without choice of frequency bands of leak signal [15], [16], which employs an adaptive filter instead of the GCC method for TDE. The adaptive filter can be updated iteratively by using the leak signal's characteristics, where the correlation function can be directly obtained from its own system parameters instead of any prior knowledge. However, the LMS-TDE is a biased estimate, and the Cramer-Rao Bound indicates that LMS error between the estimated and the true value is inversely proportional to the SNR of a signal [17]. The lower the SNR is, the greater the error of LMS-TDE based leak location method will have, which is limited to low SNR for its application of WSP.

When a leak occurs, escaping water from pipelines generate turbulence, friction and random shocks which result in dispersive, multimodal, attenuation and non-stationary acoustic vibration signal immersed in a highly noisy environment due to traffic, mechanical devices, turbulence, etc., which will bring about such a low SNR of leakage signal that the LMS-TDE based leak location method cannot be used effectively in WSP. Wavelet analysis can be used to suppress ambient noise (such as traffic noises) for leak detection in WSP, which requires adaptive selection of an appropriate mother wavelet according to the nature of leak signal and ambient noise [18]. However, the feature of leak signal and ambient noise changes with the pipeline situation and surroundings, which is impossible to predict the feature for adaptive selection of appropriate mother wavelet. If the selected mother wavelet is unsuitable, it is also impossible to remove unwanted noises from leak signals. The wavelet noise cancellation method depends on empirical parameters which are varied with pipeline situations and surroundings. Thus, empirical mode decomposition (EMD) based leak location is proposed for WSP which is a form of adaptive signal decomposition independent of base function [19]–[21]. As the EMD process depends on the nature of the signal, there is no need to manually select the basis function, which has been extensively applied in many fields such as mechanical fault diagnosis and electroencephalo-graph (EEG) processing. However, EMD still possesses some inherent drawbacks such as mode-mixing effect, end effect, etc. [22]–[24]. In order to overcome shortcomings of EMD, Wang proposed improved adaptive multipoint optimal minimum entropy deconvolution adjusted (MOMEDA) fault diagnosis method [25] and enhanced method to makes LMD overcome the mode mixing and reduce the reconstruction error for fault diagnosis of gearbox [26]. The VMD is a new non-stationary signal processing method proposed in 2014, which can self-adaptively decompose non-stationary signals through an iterative search for an optimal solution [27], [28]. Compared to EMD, multi-component signals can be non-recursively decomposed by VMD into a number of components which can control decomposition convergence conditions [29]. Hence, the decomposition process of VMD can effectively eliminate the mode-mixing phenomenon with good noise immunity. However, VMD needs to determine the decomposition number of the IMF and the penalty factor in advance which directly affects decomposition accuracy. Wang proposed the VMD parameter optimal method through normalization for improvement of VMD in gearbox fault diagnosis [30].

When a leakage-induced vibration signal is decomposed into several IMFs by VMD, only those IMFs with high SNR can be used for leak location, where the other IMFs will still generate large leak location errors. Therefore, it is necessary to propose a modified VMD method to select effective IMFs for reducing leak location errors in WSP. Considering the problem of large leak location errors with low SNR, leak location based on PDS-VMD is proposed for WSP in this work where there is no requirement to know the characteristics of leak signals in advance. VMD is used to decompose the leakage signal into several IMFs. PDS and energy ratio based adaptive selection guidance is built to select effective mode components of leakage signals. The selected mode components are reconstructed to improve SNR and reduce leak location errors. To verify effectiveness, the simulation and experiment were conducted to compare the leak location errors of proposed PDS-VMD with CC and CCC-VMD.

II. PRINCIPLE OF LEAK LOCATION BASED ON TDE IN WSP

When leakage in WSP occurs, vibration signals are generated by friction and cavitation of the high-speed water jet shooting out through the leak orifice into a free space, which can be acquired by two spatially separate acceleration sensors at both ends of a suspected leak, as shown in Fig.1.

The two acquired vibration signals are mathematically modeled as

$$\begin{cases} x_1(t) = s(t) + n_1(t) \\ x_2(t) = \alpha s(t-\tau) + n_2(t) \end{cases} \tag{1}$$

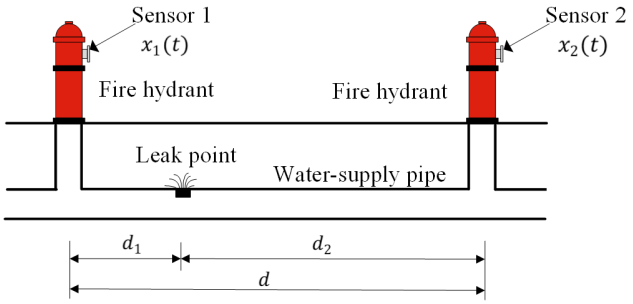

FIGURE 1. Schematic of leak location based on TDE in WSP: d is the distance between the sensor 1 and sensor 2; d_1 and d_2 are distances between leak point and sensor 1, sensor 2 respectively.

In equation (1), $x_1(t)$ and $x_2(t)$ represent the collected signals by the two sensors, $s(t)$ is the original leak source signal and unknown beforehand, $n_1(t)$ and $n_2(t)$ are zero-mean random environmental noises, α is a magnitude or power attenuation factor due to signal propagation path difference and τ is the time delay between the $x_1(t)$ and $x_2(t)$. Among them, $s(t)n_1(t)$ and $n_2(t)$ are assumed to be uncorrelated. Hence, the leak location model based on TDE is

$$d_1 = \frac{d + c\tau}{2} \tag{2}$$

In equation (2), c is the propagation speed of the vibration signal in the monitored WSP. It can be determined from equation (2) that determination of leakage position requires the propagation speed c, the distance d between the sensor 1 and sensor 2 and time delay τ of the two collected vibration signals which can be determined by CC-based TDE:

$$R_{x_1x_2}(\tau) = E\left[x_1(t)\, x_2(t-\tau)\right] \tag{3}$$

$$\tau = arg\ max\ R_{x_1x_2}(\tau) \tag{4}$$

where *arg max* represents argument of maximum CC function $R_{x_1x_2}$ and E is expectation operator.

The distance d between the two sensors can be measured in the field or determined by a known pipeline profile. The propagation velocity c is closely related to the material of pipe wall, in-pipe fluid, external environment and geometric structure size, which can be estimated by the theoretical model. Therefore, the key to leak location is to determine the time delay which is usually calculated by the formula (3) and (4). However, the errors of leak location based on CC will increase with reduction of SNR. When the SNR is low enough, the leak position cannot be determined using CC based TDE. Accordingly, a new location scheme under low SNR is desirable for WSP.

III. PRINCIPLE OF LEAK LOCATION BASED ON PDS-VMD IN WSP

A. THE PRINCIPLE OF VMD

VMD is proposed by Konstantin Dragomiretskiy *et al.* in 2014 [27], which is a new self-adaptive signal processing method and can effectively eliminate modal aliasing compared to the EMD method. The VMD method achieves self-adaptive modal decomposition through construction and solution of variational problems. Any signal can be written as the following form:

$$x(t) = \sum\nolimits_k u_k(t) \tag{5}$$

In equation (5), $u_k(t)$ is a component of the signal being decomposed, which can be defined as a frequency-modulation–amplitude-modulation (AM–FM) signal and mathematical expressed as follows:

$$u_k(t) = A_k(t)\cos(\varphi_k(t)) \tag{6}$$

In equation (6), $A_k(t)$ is the instantaneous amplitude. The instantaneous frequency $\omega_k(t)$ can be given by $\omega_k(t) = \frac{d\varphi_k(t)}{dt}$

The decomposition process of the signal using VMD is converted into the variational framework and thus, an optimal-solution processing for a constrained variational process [31] can be mathematical expressed for the constrained variational model as follows:

$$\min_{\{u_k\},\{\omega_k\}} \left\{ \sum_k \left\| \partial_t \left[\left(\delta + \frac{j}{\pi t} \right) u_k(t) \right] e^{j\omega_k t} \right\|_2^2 \right\} \tag{7}$$

In equation (7), $\{u_k\} = \{u_1, \cdots, u_k\}$ and $\{\omega_k\} = \{\omega_1, \cdots, \omega_k\}$ represent k components and the center frequency of each component respectively, following decomposition by VMD.

During VMD implementation, the constrained-variation problems can be transformed into an unconstrained variation problem with introduction of augmented Lagrange function, which is mathematicaly expressed as:

$$\begin{aligned} &L(\{u_k\}, \{\omega_k\}, \lambda) \\ &= \alpha \sum_k \left\| \partial_t \left[(\delta(t) + j\pi t) u_k(t) \right] e^{-j\omega_k t} \right\|_2^2 \\ &\quad + \left\| x(t) + \sum_k u_k(t) \right\|_2^2 + \left\langle \lambda(t), x(t) - \sum_k u_k(t) \right\rangle \end{aligned} \tag{8}$$

In equation (8), α is the penalty parameter and λ is the Lagrange multiplier. In order to obtain an optimal solution, the alternate direction method of multipliers can be applied to calculate the saddle point of the augmented Lagrange function, which is the optimal solution of the constrained-variation equation [32]. The saddle point problem is solved by the alternate renewal of u^{n+1}, ω_k^{n+1}, and λ^{n+1} are as follows:

$$\begin{aligned} u_k^{n+1} = \underbrace{argmin}_{uk \in X} \Bigg\{ &\alpha \left\| \partial_t \left[(\delta(t) + j/\pi t) u_k(t) \right] e^{-j\omega_k t} \right\|_2^2 \\ &+ \left\| x(t) + \sum_i u_i(t) + \lambda(t)/2 \right\|_2^2 \Bigg\} \end{aligned} \tag{9}$$

$$\omega_k^{n+1} = \underbrace{argmin}_{\omega k} \left\{ \left\| \partial_t \left[(\delta(t) + j/\pi t) u_k(t) \right] e^{-j\omega_k t} \right\|_2^2 \right\} \tag{10}$$

In equations (9) and (10), $\omega_k = \omega_k^{n+1}$, $\sum_i u_i(t) = \sum_{i\neq k} u_i(t)^{n+1}$.The Parseval/Plancherel Fourier isometric transformation can be used to transform equations (9) and (10) into frequency domain, thus updating the center frequencies of the modes, which can be expressed as [27]:

$$\hat{u}_k^{n+1}(\omega) = \frac{\hat{x}(\omega) - \Sigma_{i\neq k}\tilde{u}_i(\omega) + \hat{\lambda}(\omega)/2}{1 + 2\alpha\,(\omega - \omega_k)^2} \tag{11}$$

$$\omega_k^{n+1} = \frac{\int_0^\infty \omega \left|\hat{u}_k(\omega)\right|^2 d\omega}{\int_0^\infty \left|\hat{u}_k(\omega)\right|^2 d\omega} \tag{12}$$

In equation (12), $\hat{u}_k(\omega)$ is equal to Wiener filter of $\hat{x}\,(\omega) - \sum_{i\neq k}\hat{u}_i\,(\omega)$. The gravity center of the current modal function power spectrum in equation (12) is ω_k^{n+1}, and the real part of $\left\{\hat{u}_k(\omega)\right\}$ is conducted by inverse Fourier transform (IFT) to obtain $\{u_k(t)\}$.

The VMD algorithm continuously updates the modes in the frequency domain, and finally transforms them into time domain through IFT. The specific algorithm is as follows:

Algorithm 1 VMD $(x(t))$

Input: $x(t)$
Output: $\{u_k(t)\}$, $\{\omega_k\}$
Initialize $\left\{\hat{u}_k^1\right\}$, $\left\{\omega_k^1\right\}$, $\hat{\lambda}^1$, $n \leftarrow 0$
Repeat
$n \leftarrow n + 1$
for $k = 1 : K$ **do**
Update $\hat{u}_k$ for all $\omega \geq 0$:
$\hat{u}_k^{n+1}\,(\omega) \leftarrow \frac{\hat{x}(\omega) - \sum_{i<k}\hat{u}_i^{n+1}(\omega) - \sum_{i>k}\hat{u}_i^n(\omega) + \hat{\lambda}^n(\omega)/2}{1+2\alpha(\omega-\omega_k^n)^2}$
Update ω_k :
$\omega_k^{n+1} \leftarrow \frac{\int_0^\infty \omega\left|\hat{u}_k^{n+1}(\omega)\right|^2 d\omega}{\int_0^\infty \left|\hat{u}_k^{n+1}(\omega)\right|^2 d\omega}$
End for
Dual ascent for all $\omega \geq 0$:
$\hat{\lambda}^{n+1}\,(\omega) \leftarrow \hat{\lambda}^n\,(\omega) + \tau\left(\hat{x}\,(\omega) - \sum_k \hat{u}_i^{n+1}\,(\omega)\right)$
Until convergence: $\sum_k \left\|\hat{u}_k^{n+1} - \hat{u}_k^n\right\|_2^2 / \left\|\hat{u}_k^n\right\|_2^2 < \epsilon$
$u_k\,(t) = IFT\left(real\left(\hat{u}_k^{n+1}\,(\omega)\right)\right)$
Return $\{u_k(t)\}$, $\{\omega_k\}$.

B. PDS-BASED ADAPTIVE SELECTION ALGORITHM OF SENSITIVE MODE COMPONENTS

The acquired leakage vibration signals are decomposed into multiple intrinsic mode components using the VMD algorithm, where only some mode components are sensitive components containing useful information (non-dispersive and single mode) for leak location in WSP, while other mode components are not related to leakage or interferences, dispersive modes resulting low SNR and larger leak location errors. Therefore, it is necessary to propose a modal selection algorithm to extract high SNR and non-dispersive modes for reducing leak location errors. Recently, correlation coefficient based adaptive selection of sensitive modes has been proposed for intrinsic mode of EMD [20] and VMD [31] for leak location in pipelines, which can filter mode components unrelated with leakage to improve SNR and reduce leak location errors. However, collected leakage vibration signals can not only contain unrelated noise but also a related dispersive mode resulting in larger leak location errors. Hence, the adaptive selection algorithm of sensitive mode components based on PDS of cross spectrum of two collected leakage vibration signals is proposed in this work to remove the unrelated and related dispersive modes for leak location in WSP.

According to Wiener-Khintchine theorem, the cross spectrum can be obtained from the CC function by Fourier transform (FT), which can be used to express correlation between $x_1(t)$ and $x_2(t)$ in the frequency domain. Hence, the cross spectrum of $x_1(t)$ and $x_2(t)$ can be derived by performing FT of equation (3):

$$C_{x_1x_2}\,(\omega) = X_1\,(\omega)\,X_2^*\,(\omega) = \alpha C_{ss}(\omega)e^{j\omega\tau} = \alpha C_{ss}(\omega)e^{j\theta_{x_1x_2}(\omega)} \tag{13}$$

In equation (13), $X_1(\omega)$ and $X_2(\omega)$ are spectrum of $x_1(t)$ and $x_2(t)$ respectively through Fourier transform (FT), where $*$ denotes complex conjugate. $C_{ss}(\omega)$ represents auto-power spectrum of leakage source signal and τ is time delay of the two collected signals. Due to small amount of collected data, in this study, the cross spectrum is estimated by the Welch mean period graph method.

Then the coherence function of $x_1(t)$ and $x_2(t)$ can be expressed as follows:

$$\gamma_{x_1x_2}(\omega) = \frac{\left|C_{x_1x_2}(\omega)\right|}{\sqrt{C_{x_1x_1}(\omega)C_{x_2x_2}(\omega)}} \tag{14}$$

In equation (14), $C_{x_1x_1}(\omega)$ and $C_{x_2x_2}(\omega)$ are auto-power spectrum of $x_1(t)$ and $x_2(t)$ respectively performed by Welch mean period graph method. The coherence function can provide a mirror to SNR and degree of correlation between two collected signals $x_1(t)$ and $x_2(t)$, which can be used to determine coherence frequency band $[\omega_{c1},\ \omega_{c2}]$ for leak location in WSP. However, the collected signals in coherence frequency band possess dispersive nature and contain dispersive mode with high SNR and degree of correlation, which results in larger leak location errors in pipelines. As dispersive mode components will lead to time delay varying with frequency ω, it is difficult to accurately estimat time delay in coherence frequency band.

According to equation (14), the phase spectrum of cross spectrum can be obtained as follows:

$$\theta_{x_1x_2}(\omega) = \omega\tau \tag{15}$$

In equation (15), the phase spectrum is linear to frequency ω in a specific frequency band, where the collected signal contains non-dispersive mode components with high SNR and then the slope of the phase spectrum is time delay τ.

As the SNR decreases, the slope of phase spectrum becomes more difficult to determine accurately. Hence, a PDS based selection of frequency band is proposed through the difference of two frames of cross-spectral phase spectrum between $x_1(t)$ and $x_2(t)$ in this paper. The PDS varies horizontally within the frequency band $[\omega_{p1},\ \omega_{p2}]$, where the collected signal possesses high SNR and non-dispersive modes. Therefore, the characteristic frequency band $[\omega_1,\ \omega_2]$ can be selected by coherence analysis in combination with PDS in which the collected signals possess high SNR and non-dispersive mode components.

Hence, the sensitive components $\{u_{isk}(\mathrm{t})\}$ of intrinsic modes $\{u_{ik}(\mathrm{t})\}$ after VMD can be selected in the determined characteristic frequency band when $i=1$ and $i=2$ corresponds to the two collected signals $x_1(t)$ and $x_2(t)$, respectively. The selection guide of sensitive mode components is formulated by

$$R_{iE} = \frac{E_{ie}}{E_{is}} \tag{16}$$

In equation (16), the R_{iE} is defined as effective energy ratio of intrinsic modes in both the characteristic frequency band and in the whole frequency band, where E_{ie} is energy of intrinsic mode in characteristic frequency band and E_{is} is for the in whole frequency band. The sensitive components can be chosen from intrinsic modes when $R_E \geq R_{Emax}/2$, where the R_{Emax} is maximum effective energy ratio among all decomposed intrinsic modes. The proposed mode components selection method can be used to extract non-dispersive modes with high SNR, which will effectively reduce leak location errors in WSP.

The PDS-based adaptive selection (AS) algorithm of sensitive mode components is summarized as follows:

Algorithm 2 $AS(x_1(t), x_2(t))$

Input: $x_1(t), x_2(t)$
Output: $\{u_{1sk}(\mathrm{t})\}, \{u_{2sk}(\mathrm{t})\}$
  $\{u_{1k}(\mathrm{t})\} \leftarrow VMD(x_1(t))$
  $\{u_{2k}(\mathrm{t})\} \leftarrow VMD(x_2(t))$
  $[\omega_{c1},\ \omega_{c2}] \leftarrow \gamma_{x_1x_2}(\omega) = \frac{|C_{x_1x_2}(\omega)|}{\sqrt{C_{x_1x_1}(\omega)C_{x_2x_2}(\omega)}}$
  $[\omega_{p1},\ \omega_{p2}] \leftarrow \theta_{x_1x_2}(\omega) = \omega\tau$
  $[\omega_1,\ \omega_2] = [\omega_{c1},\ \omega_{c2}] \cap [\omega_{p1},\ \omega_{p2}]$
  For $i = 1:2$ **do**
    For $k = 1:K$ **do**
      $R_{iE} = \frac{E_{iek}}{E_{isk}}$
    If $R_{iE} \geq R_{iEmax}/2$
      $u_{isk}(\mathrm{t}) = u_{ik}(\mathrm{t})$
    Else
      $u_{isk}(\mathrm{t}) \neq u_{ik}(\mathrm{t})$
    End for
  End for
Return $\{u_{1sk}(\mathrm{t})\}, \{u_{2sk}(\mathrm{t})\}$

C. THE PROCEDURE OF PDS-VMD BASED LEAK LOCATION METHOD

When leakage occurs in WSP, the vibration signal propagates along the pipeline discretized into several modes and is collected by two acceleration sensors on either side of leak point as shown in Fig.1. Well below the pipe ring frequency, four types of modes are responsible for most of the energy transfer [33]: three axisymmetric modes ($n = 0$) and the $n = 1$ mode, related to beam bending. Of the $n = 0$ modes, the first, termed $s = 1$, is a predominantly fluid-borne wave; the second mode, $s = 2$, is predominantly a compressional wave in the pipe shell; the third mode, $s = 0$, is a torsional wave uncoupled from the fluid. Related research results show that the $s = 1$ mode predicted to dominate over significant propagation distances approximates a non-dispersive plane wave in the water within the pipeline [34].

Then the two collected vibration signals $x_1(t)$ and $x_2(t)$ are descomposed into multiple intrinsic mode components using a VMD algorithm as shown in section 3.1. Through the adaptive selection algorithm of sensitive mode components in section 3.2, the non-dispersive modes with high SNR can be selected and reconstructed as two new signals $x_1'(t)$ and $x_2'(t)$. Finally, the time-delay τ of two new reconstructed signals can be estimated by cross-correlation analysis and then the distance d_1 between sensor 1 and leak point can be calculated using the known distance d and propagation speed c, according to equation (2). The distance d can be measured in advance and the propagation speed c of non-dispersive $s = 1$ mode can be calculated using theoretical model [35]:

$$c = c_w \left(1 + \frac{2Ba}{E_w h - \omega^2 \rho h a^2}\right)^{-1/2} \tag{17}$$

In equation (17), c_w is the acoustic speed in a free water. The B and E_w are bulk modulus of the in-pipe water and Young's modulus of pipe wall material respectively. ρ is density of pipe wall material. The a and h are the radius and thickness of the pipe wall respectively.

The procedure of PDS-VMD based leak location method (Locator) is summarized as follows:

Algorithm 3 $Locator(x_1(t), x_2(t), d, c)$

Input: $x_1(t), x_2(t), d, c$
Output: d_1
Initialize d, c
  $\{u_{1sk}(\mathrm{t})\}, \{u_{2sk}(\mathrm{t})\} \leftarrow AS(x_1(t), x_2(t))$
  $x_1'(t) = \sum u_{1sk}(\mathrm{t})$
  $x_2'(t) = \sum u_{2sk}(\mathrm{t})$
  $R_{x_1'x_2'}(\tau) = E\left[x_1'(t)\, x_2'(t-\tau)\right]$
  $\tau = \arg\max R_{x_1x_2}(\tau)$
  $d_1 = \frac{d+c\tau}{2}$
Return d_1

The implementation steps of the proposed leak location algorithm are as follows:

(1) The characteristic frequency band of the leakage signal is determined using the cross-spectral analysis of the collected signals $x_1(t)$ and $x_2(t)$.

(2) The number of decomposition layers K of VMD is initialized to 2 and the penalty factor α is set to 2000. Then the collected leakage signals are decomposed into several modes using initialized VMD according to Algorithm 2.

(3) Let the VMD decomposition layers $K = K + 1$, repeating the step of VMD until the center frequency of the neighboring IMF components obtained by the VMD decomposition is very close, which is judged to be over-decomposed and the number of decomposition layer is determined as K.

(4) The sensitive IMF components are selected using effective energy ratio of intrinsic modes in both the characteristic frequency band and in the whole frequency band formulated by equation (16) according to algorithm 2.

(5) The sensitive components are reconstructed into two new signals $x_1'(t)$ and $x_2'(t)$.

(6) The time delay is estimated using cross-correlation analysis of two new reconstructed signals according to equation (3-4) and then the leakage is located by equation (2) and (17).

IV. THE PERFORMANCE VALIDATION OF PDS-VMD BASED LEAK LOCATION METHODS USING SIMULATION EXPERIMENTS

In order to verify the performance leak location method in low SNR, the proposed PDS-VMD, CC and CCC-VMD based leak location methods are compared in different SNR using simulation experiments. The leakage source signal $s(t)$ is simulated by Gaussian white noise through a band-pass filter of 300-400 Hz. $n_1(t)$ and $n_2(t)$ are uncorrelated by Gaussian white noise. Hence, the two collected vibration signals $x_1(t)$ and $x_2(t)$ can be generated by adding different SNR (−2dB-8dB) Gaussian white noise. The sample frequency and time delay are set as 6554 Hz and 7.629 ms.

According to the procedure of the PDS-VMD based leak location method, the two collected signals need to be decomposed into multiple modes by VMD as shown in Fig.2. The simulated signal $x_1(t)$ under SNR of 1dB is decomposed into six intrinsic mode functions (IMFs), where the frequency spectrum characteristics of each IMF are displayed in Fig.2. It can be seen that different IMFs have different frequency bands, where the frequency band of IMF1 concentrate on 300-400 Hz. This is consistent with the source signal. Therefore, the source signal can be extracted by VMD of the simulated signal.

In order to select sensitive mode components, the coherence function and PDS of two simulated collected signals are demonstrated in Fig.3. It is apparent that the cross-spectral phase difference spectrum varies horizontally in the frequency band of 300-400 Hz in subgraph where the coherence function has a maximum value. The subgraph gives details of the horizontal change of the cross-spectral phase difference spectrum in the frequency band of 300-400 Hz. Therefore the characteristic frequency band can be determined

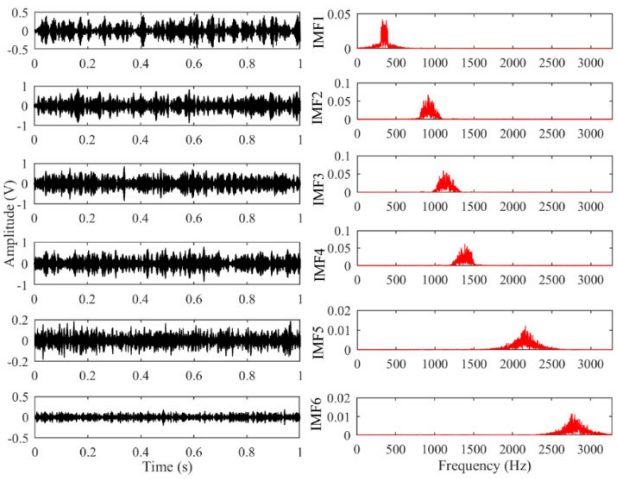

FIGURE 2. The VMD of simulated signal $x_1(t)$ and frequency spectrum analysis of each IMF.

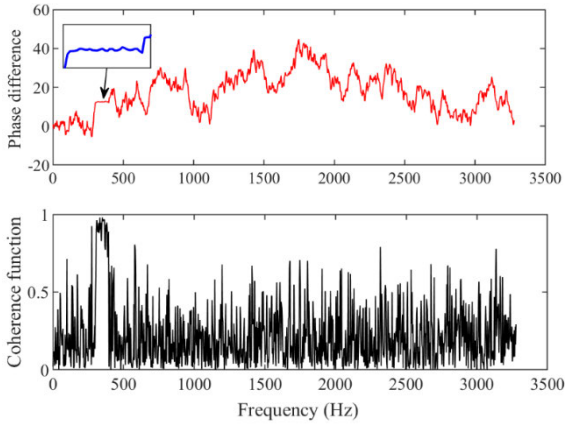

FIGURE 3. The cross-spectral phase difference spectrum and coherence function between the two simulated collected signals $x_1(t)$ and $x_2(t)$.

as 300-400 Hz by combining the phase difference and the coherence function.

Correspondingly, the effective energy ratio of the six IMFs for two simulated signals $x_1(t)$ and $x_2(t)$ in the characteristic frequency band can be calculated using Eq. (16) as shown in both Table 1 and Table 2. According to the sensitive mode selection guide, IMF1 will be chosen for both two simulated signals $x_1(t)$ and $x_2(t)$, respectively. Following this, the reconstructed signals $x_1'(t)$ and $x_2'(t)$ can be obtained by the selected IMF1. Hence, the two reconstructed signals are analyzed using cross correlation. The time delay estimation is −7.629 ms and its time-delay estimation error is 0. Accordingly, the maximum value of cross-correlation coefficient reaches up to 0.3546.

In the same manner, time-delay estimation using CC and CCC-VMD can be obtained and compared with PDS-VMD, determining relative estimation errors and degree of correlation by the cross-correlation coefficient shown in Fig.4. The figure shows the time-delay estimation error as 12.5114 ms, 4.5774 ms and 0 ms using CC, CCC-VMD and PDS-VMD,

TABLE 1. Effective energy ratios of IMF components of $x_1(t)$.

Mode	IMF1	IMF2	IMF3	IMF4	IMF5	IMF6
Effective energy ratios (%)	62.47	0	0	0	0	0

TABLE 2. Effective energy ratios of IMF components of $x_2(t)$.

Mode	IMF1	IMF2	IMF3	IMF4	IMF5	IMF6
Effective energy ratios (%)	63.04	0	0	0	0	0

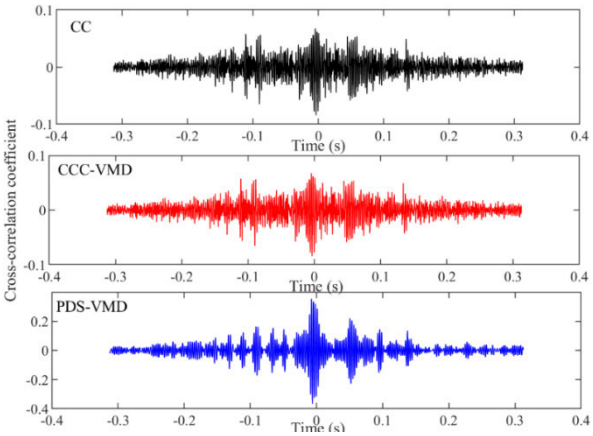

FIGURE 4. The cross-correlation coefficient of the two reconstructed signals by CC, CCC-VMD and PDS-VMD

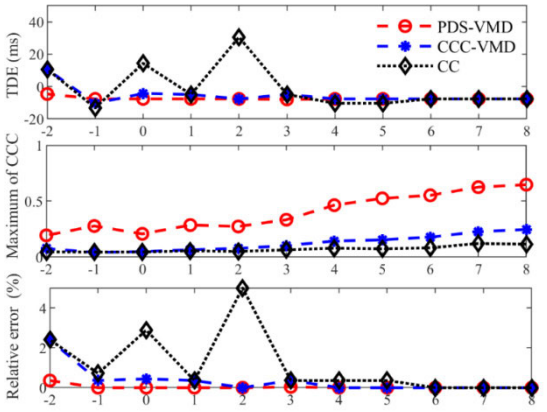

FIGURE 5. The results of time-delay estimation under different SNR from −2dB to 8dB in frequency band of 0-1.5 kHz.

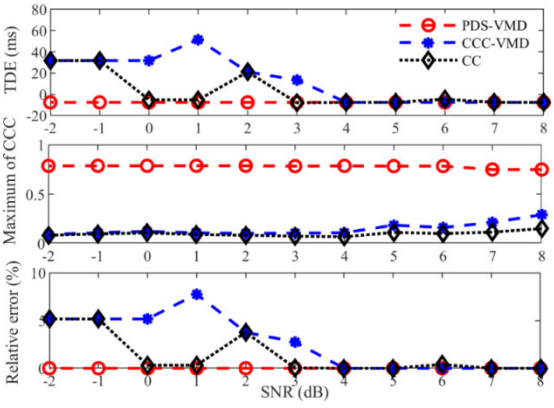

FIGURE 6. The results of time-delay estimation under different SNR from −2dB to 8dB in frequency band of 800-1500 Hz.

respectively. The cross-correlation coefficient of the two simulated signals is 0.052, 0.0676 and 0.3546 using CC and CCC-VMD and PDS-VMD respectively, which demonstrates that the PDS-VMD and CCC-VMD can improve the degree of correlation and thus reduce the time-delay estimation error.

In order to verify the performance of the proposed leak location method under broadband noise sources with different SNR in a whole frequency band compared to CC and CCC-VMD, the time-delay estimation results of the three methods were obtained under the SNR ranging from −2dB to 8dB in a frequency band of 0-1.5 kHz as shown in Fig.5. The cross-correlation coefficient of PDS-VMD is larger than that of CCC-VMD, whereby CC is the smallest, indicating that the two reconstructed signals in PDS-VMD method have the greatest relevance. Results also show that degree of correlation between the two reconstructed signals by PDS-VMD and CCC-VMD is improved compared to that using direct cross correlation when there exists broadband noise with different SNR. Therefore, the leak location method of PDS-VMD has the smallest relative errors, which of CC has the largest relative error. This suggests that the ability to be immune to noise using PDS-VMD and CCC-VMD has been improved in comparison with using direct CC.

In order to verify the performance of the proposed leak location method under narrow band noise source with different SNR in a specific frequency band of 800-1500 kHz compared to CC and CCC-VMD, time-delay estimation results of the three methods are obtained under the SNR ranging from −2dB to 8dB in a frequency band of 800-1500 kHz as shown in Fig.6. The cross-correlation coefficient of PDS-VMD is larger than both CCC-VMD and CC, whereby CC is the smallest, indicating that the two reconstructed signals in the PDS-VMD method have the greatest relevance. The degree of correlation between the two reconstructed signals by PDS-VMD and CCC-VMD have all been improved compared to using direct CC when broadbad noise source exists with different SNR. Therefore, the leak location method of PDS-VMD has the smallest relative errors and CCC-VMD has the largest relative error. This suggests that the ability to be immune to narrow band noise using PDS-VMD has been improved in comparison with using direct CC and CCC-VMD.

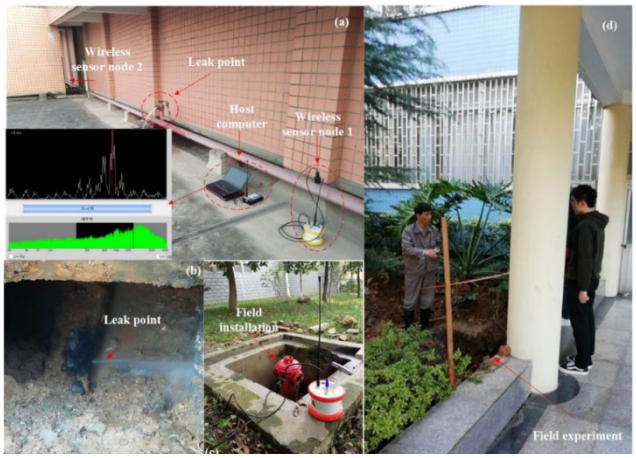

FIGURE 7. The photos of experiment for leak detection and location in the water supply pipelines: (a) experimental setup; (b) leakage position; (c) filed installation position; (d) field experiment site.

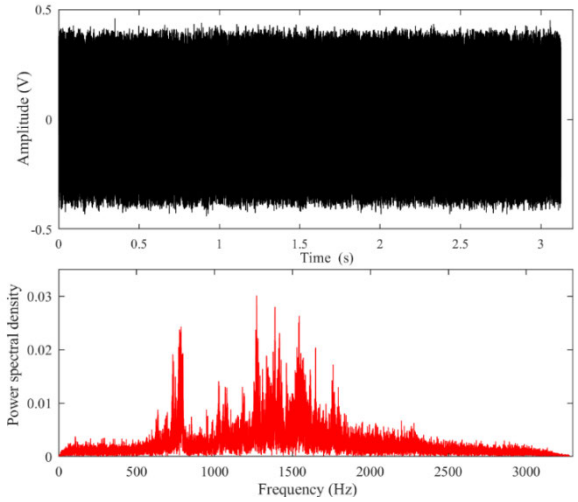

FIGURE 8. The collected vibration signal in time and frequency domain.

In summary, the simulation experiment demonstrated that the degree of correlation between two reconstructed signals by PDS-VMD and CCC-VMD is improved in comparison with using direct CC. At the same time, the PDS-VMD has the maximum suppression ability and thus the smallest TDE errors for both broadband and narrow band noise source with different SNR ranging from -2dB to 8 dB. However, the CCC-VMD has a better immunity to broadband noise source with different SNRs and worse immunity to narrow band noise source than CC.

V. EXPERIMENTS OF LEAK LOCATION IN WSP USING CC, CCC-VMD AND PDS-VMD

A. EXPERIMENTAL SETUP

The experimental setup consisted of two wireless acceleration sensor nodes and a host computer as shown in Fig.7. The two wireless acceleration sensor nodes employed a 433 MHz carrier for sending and receiving vibration data over a range of 2 km, wich was mounted on the pipe wall and collect the vibration signal with a sampling rate of 6554 Hz and synchronization acquisition accuracy of $\pm 30\,\mu s$. The host computer was installed with data acquisition and analysis software to receive and store the collected vibration data. At the same time, the host computer could control the two wireless acceleration sensor nodes to collect data synchronously and perform analysis and process of the data.

In the experiment, the underground and aboveground water-supply pipelines were chosen with a pipe wall material of nodular cast iron and a radius of 100 mm under the pressure ranges of 0.2-0.4 MPa. A fire hydrant in aboveground water pipelines were used to simulate a leak point for the leak detection and location experiment. A real leak point in underground water pipelines was also used for the experiment as shown in Fig.7.

B. EXPERIMENTAL RESULTS AND DISCUSSION

In the experiment, the collected vibration signal was aquired by two wireless acceleration sensors separated by 16 meters and then stored on a host computer. The collected vibration signals induced by water leakage in time and frequency domain are shown in Fig.8. The figure shows from the spectrum of the leakage vibration signal that the signal energy mainly concentrated in two frequency bands of 500-1000 Hz and 1000-2000 Hz. The leakage vibration signal in the frequency band of 1000-2000 Hz has the maximum energy compared to the other frequency bands.

In order to determine the leak position using the PDS-VMD method, the two collected vibraiton signals induced by water leakage were initially decomposed into six IMFs by VMD as shown in Fig.9. It can be seen that different IMFs have different frequency bands: IMF1 and IMF2 mainly concentrate on frequency band of 500-1000 Hz; IMF3, IMF4 and IMF5 mainly concentrate on frequency band of 1000-2000 Hz; IMF6 mainly concentrate on frequency band of 2000-2500 Hz.

According to the principles of PDS-VMD based leak location, decomposed IMFs by VMD need to be chosen using the sensitive mode selection guide of the PDS and coherence function to reduce leak locaiton errors in low SNR. Hence, the coherence function and PDS of two collected vibration signals are shown in Fig.10. The figure indicates that the cross-spectral phase difference spectrum varies horizontally in the frequency band of 623-778 Hz as shown in subgraph which gives details of horizontal change, where the coherence function has a larger value. Though the coherence function has a maximum value in the frequency band of 1118-1639 Hz, the cross-spectral phase difference spectrum presents a non-horizontal change, which can infer that the collected vibration signal in this frequency band possesses multimodal and dispersive components resulting in a larger TDE errors. Therefore the characteristic frequency band can be determined as 623-778 Hz by combining the phase difference and the coherence function, where the leakage vibration signal contains single non-dispersive mode approximated as a plane wave and can be used for reducing leak location errors.

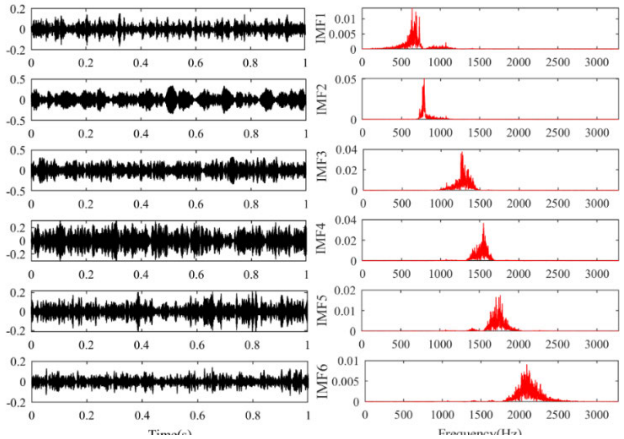

FIGURE 9. The VMD of simulated signal $x_1(t)$ and frequency spectrum analysis of each IMF.

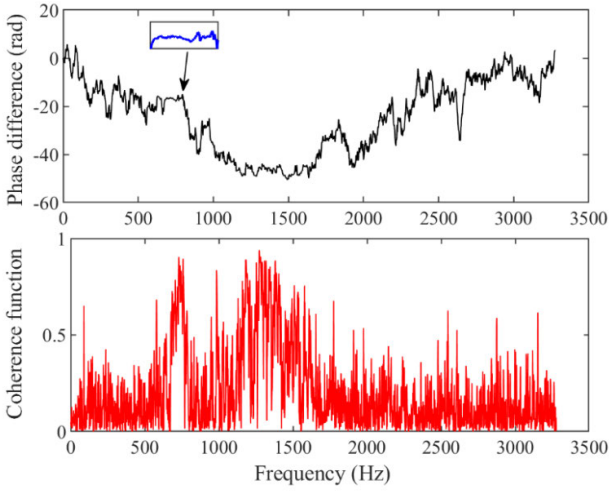

FIGURE 10. The cross-spectral phase difference spectrum and coherence function between the two collected vibration signals $x_1(t)$ and $x_2(t)$ induced by water leakage.

Correspondingly, the effective energy ratio of the six IMFs for two collected leakage vibration signals $x_1(t)$ and $x_2(t)$ in the characteristic frequency band of 623-778 Hz can be calculated using equation (16) as shown in Table 3 and Table 4. According to the sensitive mode selection guide, the IMF1 can be chosen for both two simulated signals $x_1(t)$ and $x_2(t)$ respectively. Following this, the reconstructed leakage signals $x_1'(t)$ and $x_2'(t)$ can be obtained by the selected IMF1. Hence, the two reconstructed signals can be analyzed using cross correlation to locate a leak point.The acoustic speed c is calculated as 1250 m/s using equation (17) according to the parameters of the experimental WSP. It can be obtained that the distance d_1 btween the sensor1 and leak point is 8.573 m equation (2) according to the algorithm 3 which is procedure of PDS-VMD based leak location method and the leak locaiton errror is shown to be 0.327 m using. The maximum value of cross-correlation coefficient reaches up to 0.48.

TABLE 3. Effective energy ratios of IMF components of leak signal $x_1(t)$.

Mode	IMF1	IMF2	IMF3	IMF4	IMF5	IMF6
Effective energy ratios (%)	58.57	12.26	0	0	0	0

TABLE 4. Effective energy ratios of IMF components of leak signal $x_2(t)$.

Mode	IMF1	IMF2	IMF3	IMF4	IMF5	IMF6
Effective energy ratios (%)	56.54	14.66	0	0	0	0

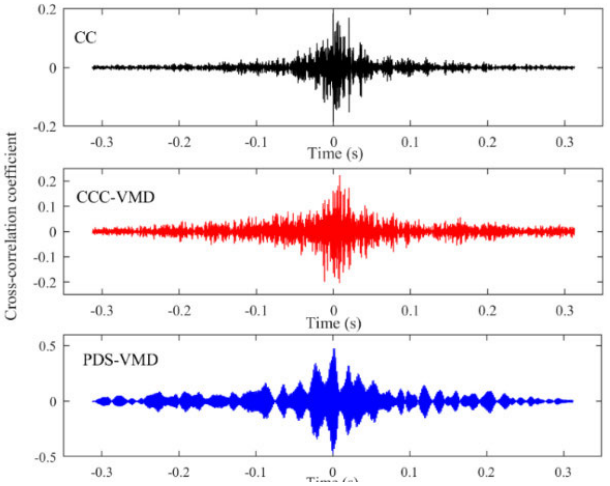

FIGURE 11. The cross-correlation coefficient of the two reconstructed leakage vibration signals by CC, CCC-VMD and PDS-VMD.

In the same way, leak location using CC and CCC-VMD can also be obtained and compared with PDS-VMD to show leak location errors and degree of correlation with cross-correlation coefficient as shown in Fig.11. This shows that leak location error is 1.09 m, 4.25 m and 0.327 m using CC, CCC-VMD and PDS-VMD respectively. The cross-correlation coefficient of the two simulated signals is 0.18, 0.22 and 0.48 using CC and CCC-VMD and PDS-VMD respectively which demonstrates that the PDS-VMD can improve degree of correlation and thus reduce time-delay estimation error effecitvely. Though the CCC-VMD also improves the correlation degree, the leak location error increases compared to that of CC, which can infer that the leakage vibration signals contains multimodal and dispersive components shown as narrow band noise.

In order to further verify the effectiveness of the proposed method, 30 groups of leakage vibration data were aquired by the two wireless sensor nodes under different distances of 16m, 20m and 20m, which are used to compare the leak location perfomance of CC, CCC-VMD and PDS-VMD. The relative leak location errors for the 30 groups of aquired data

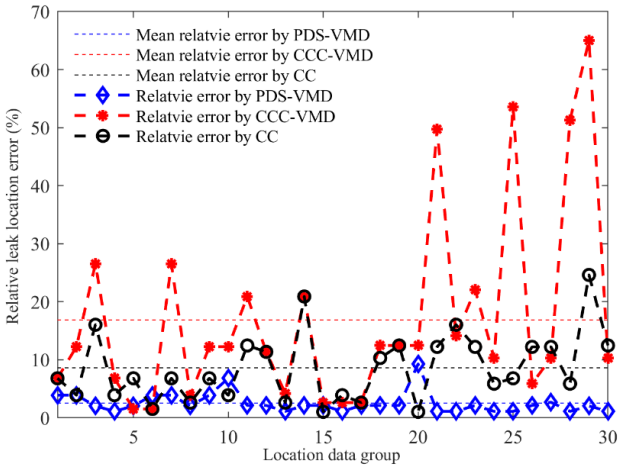

FIGURE 12. Comparison of relative errors of leak location using CC, CCC-VMD and PDS-VMD for 30 groups of leakage datas under different distances.

by CC, CCC-VMD and PDS-VMD are compared in Fig.12, which shows that the proposed PDS-VMD based leak location method has the smallest relative errror and the relative error by CCC-VMD is largest as result of multimodal and dispersive componets contained in leakage vibration signals. The average relative leak location errors are 8.62%, 16.86% and 2.53% by CC, CCC-VMD and PDS-VMD respectively. Therefore, the proposed PDS-VMD is more suitable for leak location in WSP, which is immune to both broadband and narrow band noise under low SNR.

VI. CONCLUSIONS

This work considers the problem of large leak location errors under low SNR in WSP, where the PDS-VMD based leak location method is proposed and its performance is compared with CC and CCC-VMD through the simulation and experiment, suggesting:

(1) The leakage vibration signal in WSP contains multimodal and dispersive components which can be regarded as narrowband noise resulting in low SNR and larger leak location errors. In the low frequency band of 0-1000 Hz, the leakage vibration signal contains single non-dispersive mode approximated as plane wave which can be extracted by the proposed PDS-VMD method for reducing leak location errors.

(2) The CC based leak location method is suitable for WSP under high SNR. When the SNR decreases, the leak location errors become larger. Though the CCC-VMD method will be improved the correlation degree of leakage signal under low SNR, it is sensitive to narrowband noise thus generates larger leak location errrors.

(3) The average relative leak location errors are 8.62%, 16.86% and 2.53% by CC, CCC-VMD and PDS-VMD respectively. Therefore, the proposed PDS-VMD is more suitable for leak location in WSP, which is immune to both broadband and narrow band noise under low SNR.

APPENDIX
NOMENCLATURE

CC	cross correlation
SNR	signal to noise ratio
VMD	variational mode decomposition
TDE	time-delay estimation
LMS	least mean square
EEG	electroencephalo-graph
WSP	water-supply pipelines
PDS	phase difference spectrum
IMF	intrinsic mode function
GCC	generalized cross-correlation
EMD	empirical mode decomposition
$x_1\ (t)$	collected signals by sensor 1
$x_2\ (t)$	collected signals by sensor 2
d_1	distance between leak point and sensor 1
d	distance between two sensors
$n_1(t)$	noise in $x_1\ (t)$
$n_2(t)$	noise in $x_2\ (t)$
∂	power attenuation factor
c	acoustic speed of leak signal
τ	time delay
arg max	argument of maximum function
$R_{x_1x_2}$	CC function
E	expectation operator
$u_k(t)$	component of signal
$A_k\ (t)$	instantaneous amplitude
$\omega_k(t)$	instantaneous frequency
α	penalty parameter
λ	Lagrange multiplier
$X_1(\omega)$	spectrum of $x_1(t)$
$X_2\ (\omega)$	spectrum of $x_2\ (t)$
$C_{x_2x_2}(\omega)$	auto-power spectrum
$\gamma_{x_1x_2}(\omega)$	coherence function
$\theta_{x_1x_2}(\omega)$	phase spectrum
R_{iE}	effective energy ratio
c_w	acoustic speed in a free water
B	bulk modulus of the in-pipe water
E_w	Young's modulus of pipe wall material
ρ	density of pipe wall material
a	radius of the pipe wall
h	thickness of the pipe wall

REFERENCES

[1] A. F. Colombo, P. Lee, and B. W. Karney, "A selective literature review of transient-based leak detection methods," *J. Hydro-Environ. Res.*, vol. 2, no. 4, pp. 212–227, Apr. 2009.
[2] X. Wang, J. Lin, A. Keramat, M. S. Ghidaoui, S. Meniconi, and B. Brunone, "Matched-field processing for leak localization in a viscoelastic pipe: An experimental study," *Mech. Syst. Signal Process.*, vol. 124, pp. 459–478, Jun. 2019.
[3] X. Wang and M. S. Ghidaoui, "Pipeline leak detection using the matched-field processing method," *J. Hydraulic Eng.*, vol. 144, no. 6, Jun. 2018, Art. no. 04018030.
[4] X. Wang, D. P. Palomar, L. Zhao, M. S. Ghidaoui, and R. D. Murch, "Spectral-based methods for pipeline leakage localization," *J. Hydraulic Eng.*, vol. 145, no. 3, Mar. 2019, Art. no. 04018089.
[5] H. V. Fuchs and R. Riehle, "Ten years of experience with leak detection by acoustic signal analysis," *Appl. Acoust.*, vol. 33, no. 1, pp. 1–19, 1991.

[6] O. Hunaidi and W. T. Chu, "Acoustical characteristics of leak signals in plastic water distribution pipes," *Appl. Acoust.*, vol. 58, no. 3, pp. 235–254, Nov. 1999.
[7] Y. Gao, M. J. Brennan, P. F. Joseph, J. M. Muggleton, and O. Hunaidi, "A model of the correlation function of leak noise in buried plastic pipes," *J. Sound Vib.*, vol. 277, nos. 1–2, pp. 133–148, Oct. 2004.
[8] Y. Gao, M. J. Brennan, and P. F. Joseph, "A comparison of time delay estimators for the detection of leak noise signals in plastic water distribution pipes," *J. Sound Vib.*, vol. 292, nos. 3–5, pp. 552–570, May 2006.
[9] J. Yang, Y. Wen, and P. Li, "Leak location using blind system identification in water distribution pipelines," *J. Sound Vib.*, vol. 310, nos. 1–2, pp. 134–148, Feb. 2008.
[10] J. Yang, Y. Wen, and P. Li, "The genetic-algorithm-enhanced blind system identification for water distribution pipeline leak detection," *Meas. Sci. Technol.*, vol. 18, no. 7, pp. 2178–2184, Jul. 2007.
[11] Y. Gao, M. J. Brennan, Y. Liu, F. C. L. Almeida, and P. F. Joseph, "Improving the shape of the cross-correlation function for leak detection in a plastic water distribution pipe using acoustic signals," *Appl. Acoust.*, vol. 127, pp. 24–33, Dec. 2017.
[12] F. C. L. Almeida, M. J. Brennan, A. T. Paschoalini, P. F. Joseph, and Y. Gao, "On the signum function and its effect on acoustic correlation for leak location in buried plastic water pipes," *Procedia Eng.*, vol. 199, pp. 1344–1349, 2017.
[13] M. J. Brennan, Y. Gao, P. C. Ayala, F. C. L. Almeida, P. F. Joseph, and A. T. Paschoalini, "Amplitude distortion of measured leak noise signals caused by instrumentation: Effects on leak detection in water pipes using the cross-correlation method," *J. Sound Vib.*, vol. 461, Nov. 2019, Art. no. 114905.
[14] C. Knapp and G. Carter, "The generalized correlation method for estimation of time delay," *IEEE Trans. Acoust., Speech, Signal Process.*, vol. 24, no. 4, pp. 320–327, Aug. 1976.
[15] H. Wu, Y. Wen, J. Yang, and P. Li, "Adaptive detection and location for water pipeline leaks in lower SNR and nonstationary environments," in *Proc. IEEE Int. Conf. Control Autom.*, Dec. 2009, pp. 1318–1323.
[16] H. Wu, Y. Wen, and P. Li, "Dynamic discrimination of convergence of the LMS time delay estimation in complicated noisy environments," *Appl. Acoust.*, vol. 68, no. 6, pp. 628–641, Jun. 2007.
[17] H. Steendam and M. Moeneclaey, "Low-SNR limit of the Cramer-Rao bound for estimating the carrier phase and frequency of a PAM, PSK, or QAM waveform," *IEEE Commun. Lett.*, vol. 5, no. 5, pp. 218–220, May 2001.
[18] D. Kumar, D. Tu, N. Zhu, D. Hou, and H. Zhang, "In-line acoustic device inspection of leakage in water distribution pipes based on wavelet and neural network," *J. Sensors*, vol. 2017, pp. 1–10, Oct. 2017.
[19] N. E. Huang, Z. Shen, S. R. Long, M. C. Wu, H. H. Shih, Q. Zheng, N.-C. Yen, C. C. Tung, and H. H. Liu, "The empirical mode decomposition and the Hilbert spectrum for nonlinear and non-stationary time series analysis," *Proc. Roy. Soc. London. A, Math., Phys. Eng. Sci.*, vol. 454, no. 1971, pp. 903–995, Mar. 1998.
[20] C. Guo, Y. Wen, P. Li, and J. Wen, "Adaptive noise cancellation based on EMD in water-supply pipeline leak detection," *Measurement*, vol. 79, pp. 188–197, Feb. 2016.
[21] J. Cheng, Y. Yang, and D. Yu, "The envelope order spectrum based on generalized demodulation time–frequency analysis and its application to gear fault diagnosis," *Mech. Syst. Signal Process.*, vol. 24, no. 2, pp. 508–521, Feb. 2010.
[22] D. Yu, J. Cheng, and Y. Yang, "Application of EMD method and Hilbert spectrum to the fault diagnosis of roller bearings," *Mech. Syst. Signal Process.*, vol. 19, no. 2, pp. 259–270, Mar. 2005.
[23] Y. Li, P. W. Tse, X. Yang, and J. Yang, "EMD-based fault diagnosis for abnormal clearance between contacting components in a diesel engine," *Mech. Syst. Signal Process.*, vol. 24, no. 1, pp. 193–210, Jan. 2010.
[24] Z. Shen, X. Chen, X. Zhang, and Z. He, "A novel intelligent gear fault diagnosis model based on EMD and multi-class TSVM," *Measurement*, vol. 45, no. 1, pp. 30–40, Jan. 2012.
[25] Z. Wang, W. Du, J. Wang, J. Zhou, X. Han, Z. Zhang, and L. Huang, "Research and application of improved adaptive MOMEDA fault diagnosis method," *Measurement*, vol. 140, pp. 63–75, Jul. 2019.
[26] Z. Wang, J. Wang, W. Cai, J. Zhou, W. Du, J. Wang, G. He, and H. He, "Application of an improved ensemble local mean decomposition method for gearbox composite fault diagnosis," *Complexity*, vol. 2019, pp. 1–17, May 2019.
[27] K. Dragomiretskiy and D. Zosso, "Variational mode decomposition," *IEEE Trans. Signal Process.*, vol. 62, no. 3, pp. 531–544, Feb. 2014.
[28] A. Yin and H. Ren, "A propagating mode extraction algorithm for microwave waveguide using variational mode decomposition," *Meas. Sci. Technol.*, vol. 26, no. 9, Sep. 2015, Art. no. 095009.
[29] Y. Wang, R. Markert, J. Xiang, and W. Zheng, "Research on variational mode decomposition and its application in detecting rub-impact fault of the rotor system," *Mech. Syst. Signal Process.*, vols. 60–61, pp. 243–251, Aug. 2015.
[30] Z. Wang, G. He, W. Du, J. Zhou, X. Han, J. Wang, H. He, X. Guo, J. Wang, and Y. Kou, "Application of parameter optimized variational mode decomposition method in fault diagnosis of gearbox," *IEEE Access*, vol. 7, pp. 44871–44882, 2019.
[31] Q. Xiao, J. Li, J. Sun, H. Feng, and S. Jin, "Natural-gas pipeline leak location using variational mode decomposition analysis and cross-time–frequency spectrum," *Measurement*, vol. 124, pp. 163–172, Aug. 2018.
[32] L. H. A. Maia, A. M. Abrao, W. L. Vasconcelos, W. F. Sales, and A. R. Machado, "A new approach for detection of wear mechanisms and determination of tool life in turning using acoustic emission," *Tribol. Int.*, vol. 92, pp. 519–532, Dec. 2015.
[33] J. M. Muggleton, M. J. Brennan, and R. J. Pinnington, "Wavenumber prediction of waves in buried pipes for water leak detection," *J. Sound Vib.*, vol. 249, no. 5, pp. 939–954, Jan. 2002.
[34] R. Long, M. Lowe, and P. Cawley, "Attenuation characteristics of the fundamental modes that propagate in buried iron water pipes," *Ultrasonics*, vol. 41, no. 7, pp. 509–519, Sep. 2003.
[35] S. Li, Y. Wen, P. Li, J. Yang, and L. Yang, "Determination of acoustic speed for improving leak detection and location in gas pipelines," *Rev. Sci. Instrum.*, vol. 85, no. 2, Feb. 2014, Art. no. 024901.

SHUAIYONG LI was born in Luohe, Henan, China. He received the B.Eng. degree from Xin Yang Normal University, China, in 2010, and the Ph.D. degree from Chongqing University, China, in 2014. Since 2015, he has been with the Chongqing University of Posts and Telecommunications, where he is currently an Associate Professor. His current research interests include fault diagnosis of dynamic systems, information acquisition and processing, the industrial Internet of things, and leak detection and location in fluid-filled pipelines.

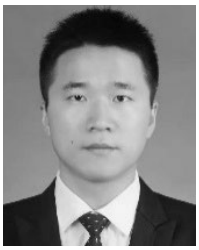

CHUANQIANG XIA was born in Sichuan, China. He received the B.Eng. degree from the Sichuan University of Science and Engineering in 2017. He is currently pursuing the M.Sc. degree with the Department of Automation, Chongqing University of Posts and Telecommunications. His main research interests include information acquisition and processing, the industrial Internet of things, and leak detection and location in fluid-filled pipelines.

ZHENHUA CHENG was born in Shandong, China. He received the B.Eng. degree from the University of Jinan, China, in 2018. He is currently pursuing the master's degree with the Chongqing University of Posts and Telecommunications. His current research interests include fault diagnosis of dynamic systems, the industrial Internet of things, and leak detection and location in fluid-filled pipelines.

WEIPEI MAO was born in Chongqing, China. He received the B.Sc. degree from Xi'an Siyuan University, in 2018. He is currently pursuing the M.Sc. degree with the Department of Automation, Chongqing University of Posts and Telecommunications. His main research interests include information acquisition and processing, the industrial Internet of things, and leak detection and location in fluid-filled pipelines.

YING LIU received the B.Eng. degree from the China University of Petroleum, Beijing, in 2015. She is currently pursuing the Ph.D. degree with the Institution of Acoustics, Chinese Academy of Sciences and School of Engineering, Edith Cowan University. Her research interests include wave propagation mechanism in cylindrical structures, including wave propagation in buried pipes and borehole acoustics for well logging.

DARYOUSH HABIBI received the Bachelor of Engineering (Electrical) degree (Hons.) and the Ph.D. degree from the University of Tasmania, in 1989 and 1994, respectively. His employment history includes Telstra Research Laboratories, Flinders University, Intelligent Pixels Inc., and Edith Cowan University, where he is currently a Professor, a Pro Vice-Chancellor, and the Executive Dean of Engineering. His research interests include engineering design for sustainable development, smart energy systems, environmental monitoring technologies, and reliability and quality of service in engineering systems and networks. He is a Fellow of Engineers Australia and the Institute of Marine Engineering, Science and Technology.